View metadata, citation and similar papers at core.ac.uk

brought to you by CORE

provided by Engineering Conferences International

Refereed Proceedings

The 12th International Conference on Fluidization - New Horizons in Fluidization Engineering

Engineering Conferences International *Year* 2007

The Effect of Vibrations on Fluidized Cohesive Powders

Diego Barletta* Giorgio Donsì† Giovanna Ferrari‡
Massimo Poletto** Paola Russo††

*University of Salerno, dbarletta@unisa.it
†University of Salerno, donsi@unisa.it
‡University of Salerno, gferrari@unisa.it
**University of Salerno, mpoletto@unisa.it
††University of Salerno, russop@dica.unisa.it

This paper is posted at ECI Digital Archives.
http://dc.engconfintl.org/fluidization_xii/45

THE EFFECT OF VIBRATIONS ON FLUIDIZED COHESIVE POWDERS

Diego Barletta, Giorgio Donsì, Giovanna Ferrari, Massimo Poletto and Paola Russo
Dipartimento di Ingegneria Chimica e Alimentare, Università di Salerno
Via Ponte Don Melillo, I-84084 Fisciano (SA), ITALY
T: +39-089-964-132; F: +39-089-964-057; E: mpoletto@unisa.it

ABSTRACT

The fluidization of a cohesive silica powder has been tested with the help of mechanical vibration. The experiments showed how the effectiveness of vibrations changed with the vibrational acceleration and frequency. The aggregative behavior of powders has been highlighted and a model procedure is proposed to predict the aggregate size starting from the measurement of powder flow properties with conventional shear testers.

INTRODUCTION

In industrial applications vibrations have been used together with fluidization in order to overcome cohesion problems arising in the treatment of sticky particles, such as those found in powder drying operations. Vibrations, in fact, are able to interact directly with structures of the dispersed phase determined by cohesive forces

Pioneering works in the field of application of vibrations to gas fluidized bed are those carried out by Gupta e Mujumdar (1), with the use of mechanical vibrations and by Morse (2) with the use of sound waves. The different effects of vibrations on group D powers reported by these two authors suggest the different mechanism of action of these two techniques. Application of sound, in particular has been proved to be very effective for the fluidization of fine powders (3, 4, 5, 6). Also mechanical vibrations were demonstrated to be effective on group C powders (7, 8, 9) by breaking the aggregates into smaller pieces which became primary particles which fluidize homogeneously as it is typical of aeratable powders.

The aggregative behavior of fine cohesive powders fluidized with vibrations has been recently described by several authors (10, 11, 12, 13) and models were proposed to evaluate the size of the aggregates in the upper layers of the fluidized beds (10) and in the freeboard (14).

The purpose of this paper is to study the effects of vibrations on the fluidization of a cohesive powder. In particular, a new model for the prediction of the aggregative behavior of these powders is proposed, which takes into account the flow properties of powders evaluated with conventional shear testers.

THEORETICAL BACKGROUND

In this paper we follow the analysis carried out by Donsì et al. (15). Their hypothesis is that during fluidization aggregates detach along the horizontal surfaces that form when the beds starts to expand. This happens when the aggregate weight overwhelms the attraction force, F_c, at the contacts between the aggregate and the upper lumps of the solids. The force balance on the detaching aggregate is:

$$\frac{\pi d_a^3}{6}\rho_a g = F_c \tag{1}$$

where g is the acceleration due to gravity, d_a and ρ_a are the aggregate diameter and density. In principle, equation (1) should also include some other force contributions accounting for fluid dynamic forces. Aggregates, however form at gas velocity much lower than those necessary for their fluidization and, therefore, fluid dynamic forces can be reasonably neglected. The value of F_c should be related to the bulk properties of the powder and, in particular, to its tensile strength. When the aggregates are touching, in fact, the relationship between the tensile stress, σ_t, and F_c might be described by the force balance across a plane separating two aggregate layers:

$$\sigma_t = F_c n_c \tag{2}$$

where n_c is the contact density between aggregates in neighboring layers that, in turn, can be expressed as:

$$n_c = k d_a^{-2} \tag{3}$$

where k is the number of the effective contacts between an aggregate and his neighbors on another layer. Empirical functions $k(\varepsilon)$ were developed for rigid spherical particles (16, 17). In that case the maximum value for k at the minimum allowed voidage was about 3. Even if for irregularly shaped aggregates the external voidage might be significantly lower than for rigid spheres, this value of k can be assumed also for the aggregates. Combining equations (1) to (3) it is possible to correlate the aggregate size starting from the bulk tensile strength of the powder:

$$\frac{\pi d_a^3}{6}\rho_a g = \frac{\sigma_t d_a^2}{k} \tag{4}$$

Given an ideal Coulomb elastic-plastic solid flow behavior, the powder yield will follow the equation:

$$\tau = \sigma \tan\phi + c \tag{5}$$

Where, σ and τ are the normal and shear stresses on the yield plane, ϕ is the angle of internal friction and c the cohesion. In this case, following the traditional Mohr-Coulomb approach, the tensile strength, σ_t, will be given by the following equation:

$$\sigma_t = -\frac{2c\cos\phi}{1+\sin\phi} \tag{6}$$

Both cohesion c and the angle of internal friction ϕ are a function0 of the powder consolidation. Assuming that this is very low inside an aerated powder, to evaluate these parameters, Donsì *et al*. (15) used the extrapolation to zero consolidation of their values measured with a powder shear tester. Furthermore, in the case of vibrated fluidization the effective acceleration is no more the acceleration due to gravity, but the effective acceleration due to vibration, a. Therefore, from equation (4) it is:

$$d_a = \frac{6}{k\pi}\frac{\sigma_t}{a\rho_a} \tag{7}$$

According to Zhou and Li (14) the aggregate density is close (about 1.15 times) to the vibrated density of the powder. In a vibrated bed, this corresponds to the density of the vibrated bed below fluidization. For simplicity, in this paper, the aggregate density, ρ_a, will be considered equal to:

$$\rho_a = m_b / H_0 \Sigma_c \tag{8}$$

where H_0 is the vibrated bed height at u = 0, m_b is the bed mass and Σ_c the column cross section. According to the experimental finding of Donsì *et al*. (15) the aggregates are visible in the initial part of the fluidization experiments and are defined by a network of cracks appearing in the fluidized bed. Given the aggregate density ρ_a the voidage external to the aggregates can be evaluated from the powder bulk density or from the bed height H:

$$\varepsilon_e = 1 - \rho_b / \rho_a = 1 - H_0 / H \tag{9}$$

In cases in which this voidage is uniformly distributed inside the fluidized bed, neglecting the gas flow inside the aggregates for their low permeability, the Ergun equation is likely to apply on the gas flow around the aggregates. The Ergun equation assumes the following form:

$$\frac{\Delta p}{H} = 150 \frac{\mu_f u}{d_a^2} \frac{(1-\varepsilon_e)^2}{\varepsilon_e^3} + 1.75 \frac{\rho_f u^2}{d_a} \frac{1-\varepsilon_e}{\varepsilon_e^3} \tag{10}$$

where u is the gas superficial velocity, μ_f and ρ_f are its viscosity and density, Δp is the pressure drop through the bed. Given the external voidage and the experimental values of pressure drops and bed heights, equation (10) can be solved to obtain an estimate of the surface to volume averaged diameter of the aggregates d_a.

EXPERIMENTAL SET UP

The core of the apparatus is a fluidization perspex column 85 mm ID and about 400 mm high fixed over an electro-dynamic vibrator, as shown in Figure 1. Details of the apparatus are given elsewhere (18).

The powder used in the experiments is a silica powder with a mean Sauter diameter of 7.6 μm with the 80% of the distribution between 2.8 and 66 μm. The effective particle density is 2650 kg m^{-3}. Desiccated air was used as fluidizing gas. Powder rheological properties were measured with a Schulze ring shear tester. Values of the powder cohesion and of the angle of internal friction relevant to fluidization were obtained by extrapolating to zero consolidation the value of these parameters from the yield loci obtained at low consolidation values. The extrapolated values are respectively 43.3 Pa for c and

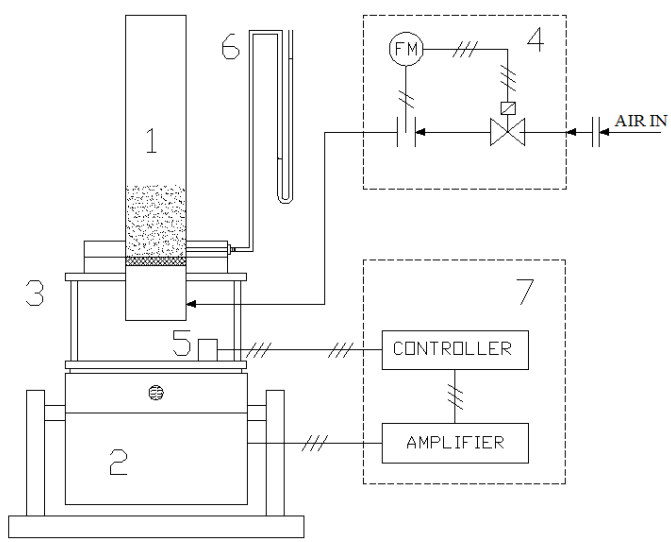

Figure 1 – Experimental apparatus: 1, fluidization column; 2, electro-dynamic vibrator; 3, metallic frame; 4, mass flow controller; 5, accelerometer; 6, water manometer; 7, vibration control block.

The 12th International Conference on Fluidization - New Horizons in Fluidization Engineering, Art. 45 [2007]

36.7° for ϕ. The value of the tensile strength, σ_t, of the powder, estimated according to equation (6), is 43.4 Pa. Details of the whole procedure are given by Donsì *et al.* (15).

All the fluidization experiments were carried out with 0.300 kg of powder. Since the initial packing state of the bed depends on its recent history, before each experiment the bed was stirred with a spoon to destroy any structures present in the powder. Then the vibration was started at the desired frequency and acceleration level. Without stopping or modifying the vibration condition, the fluidization curves were taken at stepwise increasing and, then, decreasing values of fluidization rates.

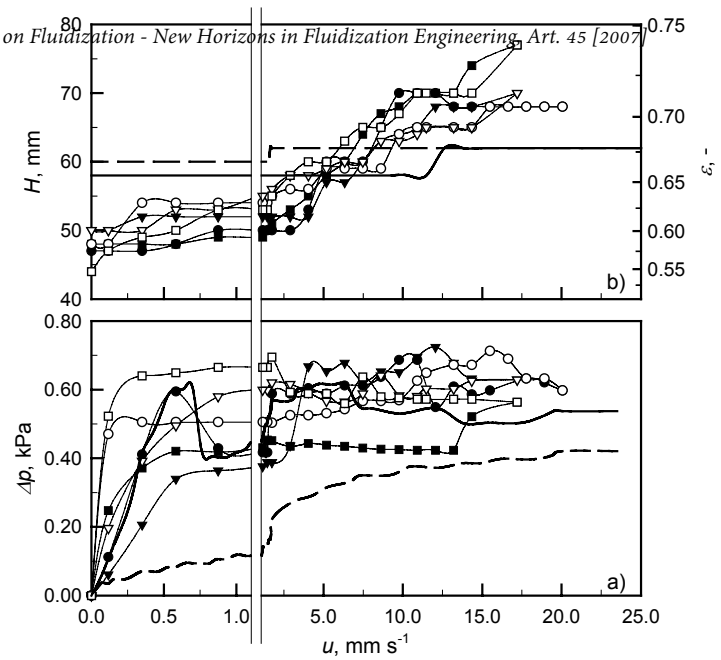

Figure 2 – Bed expansion and fluidization curves with 0.3 kg silica bed at an acceleration level *a*/*g*=2 for different vibration frequencies: ●○, 15 Hz; ▼▽, 25 Hz; ■□, 45 Hz. Filled symbols for the increasing velocity branch, hollow symbols for the decreasing velocity branch. Non-vibrated fluidization curve; ——, increasing velocity; — —, decreasing velocity.

EXPERIMENTAL RESULTS AND DISCUSSION

Applying vibrations, the maximum acceleration, *a*, is related to the vibrating sinusoidal movement. This is defined by the oscillation amplitude, *A*, i.e. half of the maximum vibration displacement, and by the oscillation frequency, *f*, or its proportional pulsation value, ω. Namely, it is:

$$a = A\omega^2 = A(2\pi f)^2 \tag{11}$$

Therefore, fixed the frequency and the maximum acceleration, the amplitude of the corresponding vibration is given by equation (11). Different acceleration levels have been chosen for the experiments. These were conventionally referred to the acceleration due to gravity, *g*, and correspond to values of *a*/*g* of 1.0, 2.0, 3.0 and 4.0.

The acceleration level for the determination of the fluidization curves shown in Figures 2 and 3 was set to the value of 2. According to some previous experiments, in fact, it was found (18) that this acceleration level was sufficient for a good vibrated fluidization of powders. The figures show the bed heights, also readable in terms of averaged voidage on the right axes, and the fluidization curves obtained bed at different vibration frequencies. Fluidization curves for frequencies of 15, 25 and 45 Hz are reported in Figure 2. Fluidization curves for frequencies of 50, 75 and 125 Hz are reported in Figure 3. Filled symbols refer to the increasing velocity branch of the fluidization curve, hollow symbols to the decreasing velocity branch. For comparison

both figures report also the non vibrated fluidization curve: the corresponding rising velocity branch is reported with a continuous thick line, the decreasing velocity branch is reported with a discontinuous thick line. Some common features of the vibrated fluidization appear clearly:

1) The average bed voidage degree reached by the vibrated bed without aeration (u = 0) is always lower than that reached without vibration.

2) The pressure drops of the fully fluidized bed with vibrations at the lowest frequencies are somewhat larger than those obtained without vibration. At the highest frequencies the vibrated fluidization pressure drops tend to assume values between those of of the increasing and decreasing branches of the non vibrated fluidization curve.

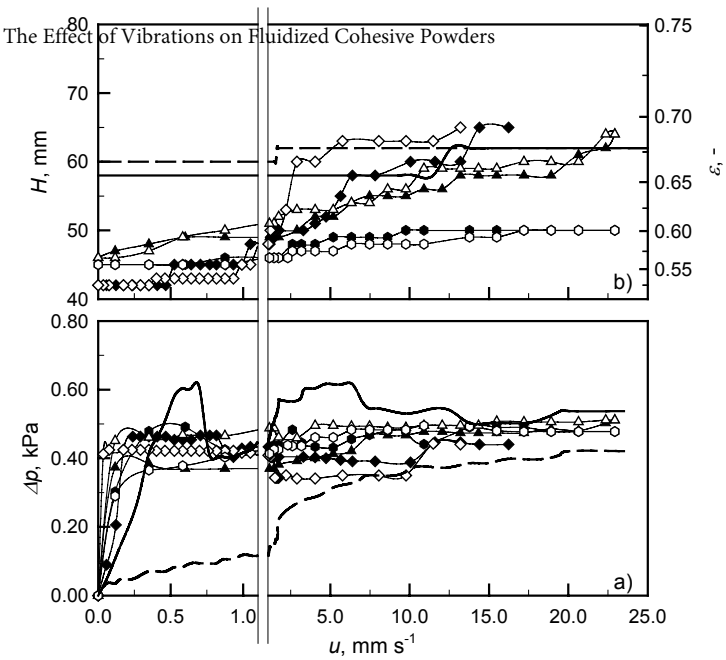

Figure 3 – Bed expansion and fluidization curves with 0.3 kg silica bed at an acceleration level a/g=2 for different vibration frequencies: ◆◇, 50 Hz; ▲△, 75 Hz; ⬢⬡, 125 Hz. Filled symbols for the increasing velocity branch, hollow symbols for the decreasing velocity branch. Non-vibrated fluidization curve; ——, increasing velocity; — —, decreasing velocity.

3) At frequencies below 80 Hz bubbling and elutriation were observed. Bubbling was very intense close to 50 Hz. In spite of this marked bed movement, the quality of pressure drop curves in figures 2 and 3 do not allow an easy identification of the minimum velocity for fluidization.

4) Vibrated fluidized beds show larger bed voidage variations than non vibrated ones. Furthermore, the maximum bed expansion obtained with vibration is generally larger than that obtained without. It tends to decrease with vibration frequencies and its value at 125 Hz is smaller than for the non vibrated bed.

5) Hysteresis of the bed expansion curve is generally less evident than the hysteresis of the fluidization curves. The largest hysteresis in the bed expansion curve is found at 50 Hz.

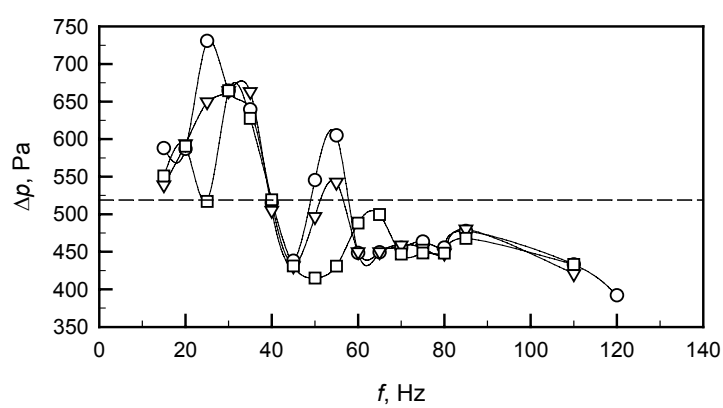

Figure 4 - Gas pressure drops as a function of vibration frequency for different fluidization velocity: □, 2.32 mm s^{-1}; ◇, 2.61 mm s^{-1}; ○, 3.18 mm s^{-1}. — — —, theoretical pressure drops at fluidization

The 12th International Conference on Fluidization - New Horizons in Fluidization Engineering, Art. 45 [2007]

The sensitivity of fluidization to bed vibration changes strongly according to the vibration frequency. As it was shown in the case of fluidized bed of powders belonging to aeratable powders (18) the frequency of the applied vibration turns out to be a key parameter in the effectiveness of the mechanical vibrations imparted to the bed by the fluidization column. Figure 4 shows the measured bed pressure drops as a function of the vibration frequency and for three different fluidization velocities. For comparison also the theoretical pressure drop coming from the bed weight is reported. Inspection of this figure and direct observation of the fluidized bed indicates that only at the lowest frequencies fluidization is helped by vibration. Vibration frequencies larger than 80 Hz bring to bed compaction and progressive bed defluidization. Direct bed observation, in particular, shows that the major bed instability is found between 45 and 50 Hz, corresponding to local maxima in Δp plots of Figure 4. This results is particularly significant if compared to the natural frequency of bed resonance calculated according to Roy et al. (19):

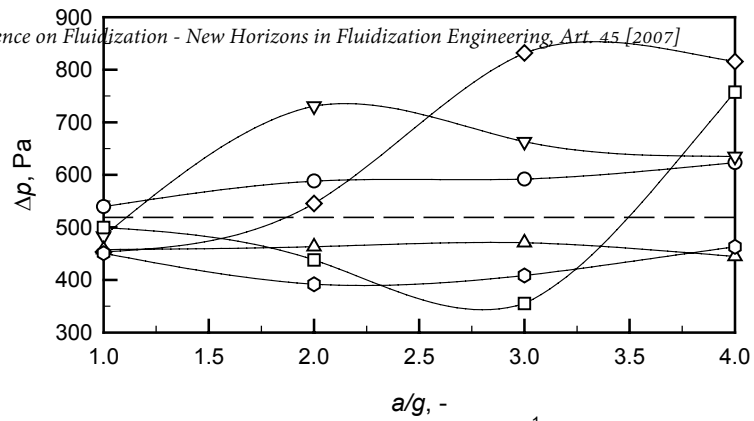

Figure 5 - Gas pressure drops (u=2.69 mm s^{-1}) as a function of vibration acceleration for different frequencies: ○, 15 Hz; ▽, 25 Hz; □, 45 Hz; ◇, 50 Hz; △, 75 Hz; ⬡, 125 Hz. — — —, theoretical pressure drops at fluidization

$$f_i = \frac{i}{4H}\sqrt{\frac{p}{\varepsilon(1-\varepsilon)\rho_p}} \qquad (i=1,3,5\ldots) \qquad (12)$$

where p is the air pressure, ρ_p is the particle density and ε the average fluidized bed voidage. Equation 12 depends on the bed expansion through the bed height and the bed voidage. Accounting for that, the frequency of the first harmonic of resonance (i=1) for the silica bed tested is between 48 Hz at the maximum bed expansion and 70 Hz at the minimum. Figure 5 shows the bed pressure drop at increasing acceleration for different vibration frequencies for a fluidization velocity u=3.18 mm s^{-1}. Plots with very similar features could be obtained at the other fluidization velocity tested (2.32 and 2.61 mm s^{-1}) and, therefore, are not reported here for conciseness. Figure 5 confirms what above said that the bed pressure drops tend to be higher at low frequencies. Bed pressure drops are also generally constant and

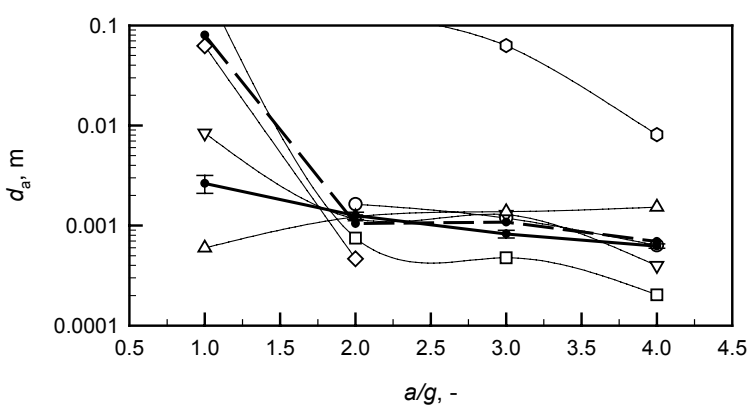

Figure 6 – Aggregate diameter as a function of vibration acceleration for different frequencies: ——, average over different frequencies of the application of equation (7). Application of equation (9): ○, 15 Hz; ▽, 25 Hz; □, 45 Hz; ◇, 50 Hz; △, 75 Hz; ⬡, 125 Hz. — — —, average over different frequencies of the application of equation (9)

do not change with the acceleration level. The only exceptions occur at the two frequencies of 45 and 50 Hz closer to the theoretical bed resonance. These results confirm the idea that the effectiveness of vibration is larger for beds close to resonant conditions.

Results of model calculation are given in Figure 6. This reports with a thick continuous line values of aggregate diameter d_a calculated according to equation (7) for different acceleration levels. In particular, application of equation (7) may bring a small dependence on vibration frequency due to different initial bed height and bed density values used to estimate the aggregate density. However, this variability is very small and it is reported with error bars of amplitude equal to twice the standard deviation. For comparison curves of aggregates diameter obtained from the application of equation (9) from fluidization experiments are reported as a function of the acceleration level and for the different frequencies tested. Each curve is the average of results obtained with experiments repeated at tree fluidization velocities (2.32, 2.61 and 3.18 mm s^{-1}). Plots relative to 50 Hz are incomplete due to the difficulty found in reading the height in a bed with a strongly oscillating surface. Inspection of the figure reveals that the agreement between the two model evaluations is satisfactory with the exception of the lowest acceleration level tested (a=1) and for the highest frequency tested. In both cases this finding can be attributed to the limited effectiveness of vibration which determines unsatisfactory fluidization. Regarding the lowest acceleration level tested (a=1) it is likely that the low effectiveness of vibrations might be due to the fact that even limited attenuation phenomena can be significant at the low accelerations. Regarding the highest frequencies, these are far from bed resonance values and the bed might not be significantly mobilized by vibration. Averages of aggregate diameters obtained at the other frequencies are reported on the thick hyphenated line, that shows a good agreement with the application of model equation (7) for acceleration levels larger than 1.

CONCLUSIONS

Some features of the fluidization of cohesive powders were observed. Some of these are shared with vibrated fluidization of aeratable powders such as the larger powder compaction of fixed beds and the larger effectiveness of vibration at frequencies close to the naturally resonant frequencies of the fluidized bed. Other are specific of cohesive powders such as the positive effect of vibrations on bed expansion. Pressure drops of vibro-fluidized beds seem to suggest a significant aggregative behavior of the powder tested and a method was developed to predict the aggregate size starting from powder flow properties characterized with a standard shear tester. Also in this case the effectiveness of vibration is closely correlated to the imparted acceleration level and to the effectiveness of powder vibration.

ACKNOWLEDGEMENTS

The authors wish to thank miss Daniela Santoro for her help with the experiments. The research reported in this paper was partially financed by the Italian Ministry of University and Research in the framework of PRIN research funding.

LIST OF SYMBOLS

A vibration amplitude, m
a acceleration due to vibration, m s^{-2}
c cohesion, Pa
f frequency, s^{-1}
F_c contact force, N
f_i resonance frequencies, s^{-1}
g acceleration due to gravity, m s^{-2}
k number of contacs, -
H bed height, m
H_0 initial bed height, m
m_b bed mass, kg
n_c contact densiy, m^{-2}
p pressure, Pa
u fluid superficial velocity, m s^{-1}

Greek symbols

Δp pressure drops, Pa
ε bed voidage, -
ε_e bed voidage around the aggreg., -
d_p aggregate diameter, m
d_p particle diameter, m
ϕ angle of internal friction, deg
μ_f fluid viscosity, Pa s
ρ_a aggregate density, kg m^{-3}
ρ_b bed density, kg m^{-3}
ρ_f fluid density, kg m^{-3}
ρ_p particle density, kg m^{-3}
σ normal stress, Pa
σ_t tensile stress, Pa
τ shear stress, Pa
ω pulsation, s^{-1}
Σ_c column cross section, m^2

REFERENCES

1. Gupta, R. and Mujumdar, A.S. 1980 *J. Chem. Eng.*, *58*, 332-338.
2. Morse, R.D. 1955 *Ind. Eng. Chem.*, *47*, 1170-1180.
3. Chirone, R., Massimilla, L. and Russo, S. 1993 *Chem. Eng. Sci.*, *48*, 41-52.
4. Russo, P., Chirone, R., Massimilla, L. and Russo, S. 1995 *Powder Technol.*, *82*, 219-230.
5. Nowak, W., Hasatani, M. and Derczynski, M. 1993 *AIChE Symp. Ser.*, *89*, 137-149.
6. Levy, E.K. Shnitzer, I. Masaki., T. and Salmento, J. 1997 *Powder Technol.*, *90*, 53-57.
7. Mawatari, Y., Koide, T., Tatemoto, Y., Uchida, S. and Noda, K. 2002 *Powder Technol.*, *123*, 69-74.
8. Mawatari, Y., Tatemoto, Y. and Noda, K. 2003 *Powder Technol.*, *131*, 66-70.
9. Marring, E., Hoffmann, A.C. and Janssen, L.P.B.M. 1994 *Powder Technol.*, 79, 1-10.
10. Xu, C. and Zu, J. 2005 *Chem. Eng. Sci.*, *60*, 6529 – 6541.
11. Xu, C. and Zu, J. 2006 *Powder Technol.*, *161*, 135 – 144.
12. Hakim, L.F., Portman, J.L., Casper, M.D. and Weimer, A.W. 2005 *Powder Technol.*, *160*, 149 – 160.
13. Valverde, J.M. and Castellanos, A. 2006 *AIChE J.*, *52*, 1705–1714.
14. Zhou, T. and Li, H. 1999 *Powder Technol.*, *101*, 57–62.
15. Donsì, G., Ferrari, G., Poletto, M. and Russo, P. 2003 *KONA*, *21*, 54-66.
16. Rumpf, H. 1962 *Agglomeration*. in W.A Knepper (ed.), Wiley, New York, 379-418.
17. Kendall, K., Alford, N.McN. and Birchall, J.D. 1987 *Proc. R. Soc. Lond.*, *A412*, 269-283.
18. Barletta, D., Donsì, G., Ferrari, G., Fusco, A., Poletto, M. and Russo, P. 2006 Proc. *5th World Conf. on Part. Technol.*, Orlando (FL), April 23-27, paper 262.
19. Roy, R., Davidson, J.F. and Tuponogov, V.G. 1990 *Chem. Eng. Sci.*, *45*, 3233-3245.